Published in: *Network*, 3:105-119, 1992.
Scanned figures supplied last.

MODELLING HEBBIAN CELL ASSEMBLIES COMPRISED OF CORTICAL NEURONS

Short title: Modelling Hebbian Cell Assemblies

A. Lansner, E. Fransén
SANS—Studies of Artificial Neural Systems
Dept. of Numerical Analysis and Computing Science
Royal Institute of Technology, S–100 44 Stockholm, Sweden
E–mail: ala@sans.kth.se

Abstract

A highly simplified network model of cortical associative memory, based on Hebb's theory of cell assemblies, has been developed and simulated. The network is comprised of realistically modelled pyramidal–type cells and inhibitory fast spiking interneurons and its connectivity is adopted from a trained recurrent artificial neural network. After–activity, pattern completion and competition between cell assemblies is readily produced. If, instead of pyramidal cells, motor neuron type cells are used, network behaviour changes drastically. For instance, spike synchronization can be observed but after–activity is hard to produce. Our results support the biological feasibility of Hebb's cell assembly theory. The analogy between this theory and recurrent artificial neural network models is discussed.

Keywords Neural modelling, cortical associative memory, recurrent artificial neural network, cell assemblies, after–activity, pattern completion, spike synchronization.

1 Introduction

1.1 Hebbian cell assemblies and models of cortical associative memory

In his classical book, The Organization of Behavior, Hebb described a functional unit which he called a cell assembly [1]. This was a group of cells strongly connected through excitatory synapses. Such an assembly could emerge as a result of repeated co–activation of its constituent cells and the action of what we today refer to as Hebbian synapses, *i.e.* excitatory synapses enhanced by co–activity of the pre– and postsynaptic neuron.

Hebb proposed that the assembly so formed thereafter could serve as an internal representation of the corresponding object in the outside world. Its existence could influence system performance and eventually explain certain perceptual phenomena, *e.g.* perceptual completion. It has later been suggested that competition between cell assemblies through lateral inhibition could explain phenomena like figure–ground separation and perceptual rivalry. Even chains of associations and, eventually, associative thought processes could be understood in terms of cell assemblies active in succession.

1.2 Earlier investigations

Hebb's original theory was mainly of a qualitative character. As such it left many things open so that mathematical modelling could be done in different ways. At the time of the first attempts to test the theory by means of computer simulations the prototypical neuron was the spinal motor neuron. Characteristics of such neurons were therefore used in early modelling work. Rochester *et.al* [2] using very simple pulse generating motor neurons with modifiable synapses failed to demonstrate the formation of Hebbian assemblies. Later MacGregor and McMullen [3] used a more realistic spiking motor neuron model. They found spike synchronization within populations of neurons with recurrent excitation, but no signs of after–activity with a duration of about 500 ms – the kind hypothesized by Hebb (ref. [1], page 74).

Hebb's cell assembly theory has been further elaborated by *e.g.* Milner [4], Braitenberg [5], and Palm [6]. It is still, in its general aspects, compatible with experimental findings relating to cortical architecture and physiology, such as for example the existence of long–ranging horizontal intracortical connections [7] and the observation of reverberating activity in short–term [8, 9] and long–term [10] memory tasks. Thus, despite the negative results from early computer simulations, the cell assembly theory has remained one of the most viable hypotheses relating to cortical function [11, 12, 13, 14].

Over the last few years, the computational advantages of neural networks of the kind suggested by Hebb has been thoroughly established in studies of abstract recurrent artificial neural network (ANN) models, *e.g.* linear [15] and binary associative memories [16] and Hopfield type networks [17, 18, 19]. Recently it has also been demonstrated that small networks of cultured cells can indeed display activity of the sort described by these computational models [20]. Furthermore, the relevance of models of this type for understanding higher cognitive brain functions was recently elaborated on in depth by Smolensky [21]. In fact, a prototypical recurrent ANN used as an auto–associative content–addressable memory (CAM) can be regarded as a mathematical realization of Hebb's basic idea. A "memory" in such a network, *i.e.* a group of units kept together by strong recurrent excitation produced by enhanced Hebbian synapses, corresponds closely to a cell assembly. The dynamic recall process converging to a low energy, stable state is analogous to the triggering of activity in a cell assembly. It is crucial to establish the relations between todays computational models and neuro–psychological theories of cortical function, since results relating to storage capacity [22, 19], prototype extraction capabilities [23] *etc.* of the former might then have a direct bearing on our understanding of cortical associative memory.

One argument against the biological relevance of Hebb's cell assembly theory has been the failure to demonstrate after–activity in populations of mutually exciting neurons by means of computer simulations. However, in some of our own early investigations, using a cell model very similar to the one of MacGregor and McMullen, after–activity could indeed be produced provided that the model motor neurons were replaced by pyramidal–cell type neurons [24]. Recently, some preliminary investigations verified these results using a more elaborate cell model [25]. The purpose of the present study was to look somewhat deeper into these issues. It should be emphasized from the start that the work presented here is not in the first place intended to be a biologically realistic model of a piece of cortex. It is rather an exploratory study of an attractor type of neural network using more realistic neurons than has commonly been the case. We believe that, despite the dramatic simplifications, this may still serve as a reasonable first step towards more

elaborate and biologically realistic models of cortical associative memory functions.

2 Cell model and cell types

Over the last few years, a general purpose simulator, SWIM, intended for numerical simulation of networks of biologically realistic model neurons, has been developed [26, 27]. The model neurons supported by SWIM can be composed of an arbitrary number of iso–potential compartments, one representing the cell body and the others the dendritic tree. Voltage dependent ion channels are modelled using Hodgkin–Huxley–like equations. Na^+, K^+, and Ca^{2+} channels are included as well as Ca^{2+} dependent K^+ channels. Two calcium pools, one fast (typical time constant 15 ms) and the other slow (typical time constant 300 ms) are modelled. When a presynaptic cell fires an action–potential a synaptic conductance opens after a conduction delay. The postsynaptic conductance increase is modelled as a square pulse and the duration used in our simulations is 3 ms. For the NMDA receptor gated synapse the magnesium block is modelled with a Hodgkin–Huxley type of equation. The combined transmitter– and voltage–dependence of the NMDA channel tends to increase the on/off behaviour of the postsynaptic cell, thus supporting the threshold nature of cell assembly activation (see sect. 4.2). Futher details regarding the cell model used here can be found elsewhere [27].

(FIGURE 1 somewhere here)

In the present study, two different types of excitatory neurons were simulated, *i.e.* the "P–cell" modelled after a typical cortical pyramidal cell and the "MN–cell" with properties derived from a motor neuron. One type of inhibitory neurons, the "FS–cell", modelled after cortical fast spiking cells [28], were used as interneurons. For the first and second cell type four compartments were used to represent the spatial extent of the neuron. In the third case only two compartments were used. Contrary to the "standard" motor neuron, the P–cell was modelled with a low firing threshold, a pronounced depolarizing after–potential (DAP), a small and late after–hyperpolarization (AHP), and a higher maximum firing frequency [29, 28, 30]. The parameters of the MN–cell were identical to those used for the excitatory interneuron in a recently studied model of the Lamprey spinal cord [27, 31]. This interneuron has properties very similar to those of spinal motor neurons. The FS–cell has a small soma, one dendritic compartment, a high maximum firing frequency and lacks an undershooting fast AHP. Appendix 1 gives the parameter values for the MN– and FS–cells. Tab. 1 gives values for the parameters in which the P–cell differ from the MN–cell. The shape of the action potentials and sample spike trains of the P–cell, MN–cell and FS–cell respectively are shown in figs. 1 a and 1 b. In fig. 2 the current–frequency response of the same cells is shown. The response of the P–cell has a highly non–linear shape whereas the MN–cell has an almost linear input–output characteristic.

(TABLE 1 and FIGURE 2 somewhere here)

3 Network architecture and connectivity

The network simulated was comprised of fifty excitatory and fifty inhibitory model neurons interacting through excitatory and inhibitory synapses. These were located on the most

distal and proximal dendritic compartments respectively. Values for synaptic strengths were adopted from a recurrent Bayesian ANN [19] trained with 8 random patterns with 8 active units in each. Pairs of patterns shared between 0 and 3 units. The Bayesian learning rule produced excitatory synapses within the patterns and inhibitory ones between them. The network can be seen as composed of fifty pairs of one excitatory cell and one inhibitory interneuron. The interneuron recieves input from excitatory cells in other pairs and inhibits its companion excitatory cell. Altogether there were 408 excitatory synapses connecting the excitatory cells, 1538 excitatory synapses from the excitatory cells to inhibitory interneurons and 50 inhibitory synapses connecting an inhibitory interneuron with its excitatory cell. The typical conduction delay was 1 ms. Synapses between the excitatory cells were of a mixed type with a conventional AMPA/kainate component and an NMDA component of equal sizes. The significance of NMDA channels has recently been investigated in the Lamprey model [32]. Mean amplitude of the EPSP:s was about 1.1 mV (range 0.01–2.0 mV) with a half–width of 36.2 ms. The synapses from an excitatory cell to an inhibitory cell were of the AMPA/kainate type with a mean value for the EPSP:s of 3.6 mV (range 0.1–6.3 mV) and a half–width of 20.9 ms. Inhibitory synapses were modelled after the conventional postsynaptic inhibition, mediated via $GABA_A$ or possibly glycine ($GABA_B$ type inhibition was not included). The strength was set to give an IPSP of -4.8 mV and the half–width was 9.7 ms. Synaptic conductances (and thus PSP amplitudes) have been exaggerated compared to values found experimentally to compensate for the small number of cells in an assembly.

In the simulations a number of excitatory cells belonging to one or several assemblies were stimulated by means of a depolarizing current injection. To avoid synchronization artifacts due to identical stimulation parameters, stimulus strengths were sampled from a normal distribution with a standard deviation of 5 percent of its mean value. Stimulus onset and duration were also randomized such that the standard deviation was matched to the interspike intervals of the active cells.

In the following, we give some results from different simulations carried out with this model. These investigations focused on (i) the ability of the network to produce after–activity; (ii) its pattern completion capabilities; (iii) competition between cell assemblies and noise suppression; (iv) spike synchronization between active cells; and (v) the significance of some specific single cell properties.

4 Simulation results

4.1 After–activity

Fig. 3 a shows the effect of stimulating all cells in an assembly comprised of P–cells as the excitatory cells with 0.4 nA for about 40 ms. For an isolated cell such a stimulation resulted in two or three spikes. Due to the mutual synaptic excitation the cells continue to fire. The firing frequency gradually decreases due to accumulated calcium entering through the Ca^{2+} channels and the NMDA channels. Calcium opens Ca^{2+} dependent K^+ channels and causes hyperpolarization which counteracts synaptic excitation. Activity terminates after about 380 ms, thus out–lasting the triggering stimulus by more than three hundred milliseconds. The duration of activity varied between 350 and 400 ms for the eight patterns stored. This is a clear demonstration of after–activity of the type suggested by Hebb. Without the slow accumulation of calcium entering through the NMDA channels

the after–activity would have persisted. Other factors than the time constants of this calcium, also influencing the duration of the after–activity, are the conductance through the Ca^{2+} dependent K^{+} channels and the magnitude of the mutual excitation between cells in one assembly.

(FIGURE 3 somewhere here)

The capability of an assembly consisting of motor neuron type cells to produce after–activity was also investigated (fig. 3 b). A large number of different experiments were carried out, *i.e.* varying stimulation strength, length, pattern and timings together with excitatory synaptic strengths. After–activity was observed only in exceptional cases, *i.e.* ordered cyclic firing of the cells, or with biologically extreme parameter values. These cases were never robust to changes in stimulation parameters. One explanation seems to be that the prominent AHP of the MN–cell to a large extent masks the EPSP produced by the mutual excitatory synapses, *i.e.* the EPSP arrives during the relative refractory period. This effect is enhanced by the tendency of the MN–cells to spike synchronize (see below) and by their high firing threshold. Our results with respects to mutually exciting motor neuron type cells confirm results from earlier simulations [3].

4.2 Pattern completion

In addition to producing sustained after–activity, mutual excitation between neurons in the cell assembly also provides the network with a capability for pattern completion. This means that when a cell assembly is only partially stimulated, the rest of its members will quickly be activated due to the strong excitatory input from the cells already firing. This was clearly demonstrated in our simulations, which also showed that triggering of activity in a cell assembly is a threshold phenomenon. Both intensity and duration of stimulation influence whether or not an assembly is activated. Fig. 4 shows the effect when a cell assembly is only partially stimulated. With two P–cells out of eight stimulated (fig. 4 a) just transient activity occurred, while with one more cell receiving stimulation (fig. 4 b) activity in the entire assembly was triggered. Qualitatively the same results were obtained when any of the other seven assemblies stored were subjected to the same tests.

If continuously stimulated (with a mean current of 1.5 nA), an assembly consisting of MN–cells also displayed some pattern completion (fig. 4 c). However, the effect was less pronounced since the cells lacking direct stimulation fired at a low rate, often just a third of that of the others.

4.3 Competition and noise suppression

There is a quite potent lateral inhibition between assemblies in our network, *i.e.* P–cells in different assemblies have strong disynaptic inhibition between them. This gives rise to competition between assemblies for total dominance of activity in the network. Fig. 4 d shows the activity resulting when two assemblies were stimulated at the same time. Five cells in the first one and three in the second one received direct input for 40 ms. It can be seen that, initially, units from both assemblies got active but after a short time the assembly receiving the most stimulation took over, thus shutting activity in the other one off completely. The winning assembly also activated its missing members. In another

simulation, when part of a cell assembly and some randomly activated cells were used as stimulus, the spurious cells were quickly silenced and the missing ones activated.

(FIGURE 4 somewhere here)

4.4 Spike synchronization

Different types of oscillatory activity and spike synchronization at various cortical locations has received much interest in recent years [33, 34, 35, 36]. As already mentioned, our simulations have showed that a group of MN–cells having mutual excitatory synapses have a tendency to spike synchronize. This can be seen in fig. 4 c where MN–cell firing is to some extent spike synchronized. The same type of synchronization has been observed among electrically coupled neurons *in vivo* [37].

Fig. 5 a shows in more detail the results obtained when a set of mutually exciting MN–cells are driven by external stimulation. In this case, both excitatory and inhibitory synapses were located at the most proximal dendritic compartment. The "synthetic field potential" showed in the figure was calculated as the average soma potential of all cells receiving inhibition from the active cells. As a control we also show the same display when the excitatory synapses were removed (fig. 5 b).

At least under the conditions studied here, the P–cell assembly did not seem to give very significant spike synchronization. Fig. 5 c shows representative traces from a simulation of a cell assembly composed of such cells. Additional experiments with the MN–cell network showed that the degree of synchronization decreased when excitatory synapses were moved further out in the dendritic tree. It was also more easily produced at low spiking frequencies and at conduction delays between cells below 3 ms.

(FIGURE 5 somewhere here)

5 Discussion

The simulation results presented in this paper show that Hebbian cell assembly related activity could readily be produced by a network with cortical pyramidal cells as the principal excitatory cells. Such a network would also display pattern completion, noise tolerance and competitive phenomena in cases of conflicting inputs in much the same way as a recurrent ANN. Clearly, the model studied here is not sufficiently sophisticated to account for any major part of the relevant experimental findings relating to cortical associative memory. It is very far from accurately describing even a small piece of real cortex. For instance, in terms of cell numbers and complexity of connectivity we are still way off from reality.

However, despite these rather drastic simplifications, the simulation results presented here can still shed some light on the neurobiological feasibility of the cell assembly theory. In addition, they have added some further details to such a theory. For instance, we may interpret our results to mean that some cortical pyramidal cell populations could have developed functional properties, *e.g.* a low firing threshold, DAP and late AHP, to support cell assembly related activity.

On the other hand, high frequency regular activity with a duration of several hundred milliseconds has rarely been observed in recordings of cortical cell activity. In a small network as the one simulated here, a high firing frequency of all cells is necessary to ensure a reliable after–activity. In a network of more realistic size, the cells may fire at a lower frequency and more irregularly during the after–activity phase. In the experimental situation, such activity would be hard to detect and identify as relating to the activity of one and the same assembly. Futhermore, in a functioning system there might well exist some reset mechanism that turns off activity in the assembly shortly after a stable attractor state has been reached, thus giving way for the activation of some other assembly.

Worth noting in this context is the rather short time required for the activation of a complete assembly. Almost without exception, even in cases of conflicting input, a clean "interpretation" was stable 50–70 ms after stimulus onset in our simulations (see *e.g.* fig. 4 d). This implies that each pyramidal cell involved needs to fire no more than about five spikes before the computation is complete. These rather impressive *reaction times* are also short enough to support sustained processing times below the 100 ms observed in some experiments on perceptual tasks *e.g.* visual object identification [38]. Thus, contrary to what is sometimes put forward, arguments relating to a too low processing speed, cannot be used to rule out recurrent attractor network models of cortical perceptual processing.

The present study also has shown that if, instead of pyramidal cells, we have motor neuron type cells connected by mutual excitatory synapses, this network has a tendency to produce spike synchronization. It does not, except within very limited or biologically extreme regions in parameter space, seem to be capable of producing sustained after–activity. However, the possibility that a large enough assembly of motor neuron type cells might still be able to display such activity is not entirely ruled out.

It should perhaps be pointed out that the spike synchronization seen in our simulations is produced merely by mutual excitation among active neurons and does not rely on feed–back inhibition which sometimes is assumed to be a necessary condition for cortical oscillatory activity. Moreover, the simulated field potential is dominated by inhibited cells.

Results produced with the motor neuron type cells are likely to transfer readily to a network of pyramidal cells with a more pronounced AHP than that of the P–cell model used here. This points towards a possible explanation for the spike synchronization and high–frequency oscillatory phenomena observed in cortex. However, further simulations that represent more accurately the geometry of large sheets of cortical tissue are required in order to elucidate whether or not these mechanisms provide a possible explanation for the synchronization observed experimentally between distant cells [34].

Taken together, the results of this simulation study point in a direction towards the reverberatory activity in cell assemblies as a principal mechanism in short–term [8, 9] and long–term [10] memory tasks. Our results also suggest that the pyramidal cell population taking part in reverberatory activity is different from the motor neuron like one that produces spike–synchronization and field potential oscillations. Even though this hypothesis appears to be biologically feasible, there is still not enough direct experimental support to allow us to select and formulate more detailed models of these processes. Further progress in our understanding of cortical associative memory mechanisms is critically dependent upon continued experimental investigations complemented by work aiming at a synthesis, involving extensive computer simulations of increasingly complex models of the underlying neuronal networks.

6 Conclusions

We have demonstrated that Hebbian cell assembly related activity can be robustly produced under some biologically reasonable assumptions. One important prerequisite is that the model of the excitatory neurons used is provided with properties of cortical pyramidal cells rather than spinal motor neurons. The former ones typically show a low firing threshold, a depolarizing after potential and a small and late AHP in comparison to the latter ones. Our simulation results support the biological feasibility of Hebb's cell assembly theory and could eventually provide a bridge between recurrent artificial neural network models and biological models of associative memory.

Our future research will be concerned with making this model more elaborate and realistic than is presently the case. The number of neurons in the simulated network will become much larger and the complexity of the connectivity will be increased. The extended model will be simulated on a Connection Machine (a massively parallel computer) using the simulator program BIOSIM [39].

7 Acknowledgment

Valuable comments on the manuscript by Sten Grillner, Per Hammarlund, Tom Wadden, Örjan Ekeberg and Lennart Brodin are gratefully acknowledged. This work was supported by the Swedish National Board for Technical Development (STU), grant no. 87–00321P.

References

[1] Hebb, D. O. *The Organization of Behavior.* John Wiley, New York, 1949.

[2] Rochester, N., Holland, J., Haibt, L., and Duda, W. Tests on a cell assembly theory of the action of the brain, using a large digital computer. *IRE Trans. Information Theory*, IT–2:80–93, 1956.

[3] MacGregor, R. and McMullen, T. Computer simulation of diffusely connected neuronal populations. *Biol. Cybernetics*, 28:121–127, 1978.

[4] Milner, P. M. The cell assembly: Mark II. *Psychol. Rev.*, 64:242–252, 1957.

[5] Braitenberg, V. Cell assemblies in the cerebral cortex. In Heim, R. and Palm, G., editors, *Theoretical approaches to complex systems*, pages 171–188. Springer Verlag, 1978.

[6] Palm, G. *Neural Assemblies. An Alternative Approach to Artificial Intelligence.* Springer Verlag, Berlin, 1982.

[7] Gilbert, C. D., Hirsch, J. A., and Wiesel, T. N. Lateral interactions in visual cortex. In *Cold Spring Harbor Symposia on Quantitative Biology*, volume LV, pages 663–676. Cold Spring Harbor Laboratory Press, 1990.

[8] Miyashita, Y. and Chang, H. S. Neuronal correlate of pictorial short–term memory in the primate temporal cortex. *Nature*, 331:68–70, 1988.

[9] Funahashi, S., Bruce, C. J., and Goldman-Rakic, P. S. Visuospatial coding in primate prefrontal neurons revealed by oculomotor paradigms. *J. Neurophysiology*, 63(4):814–831, 1990.

[10] Miyashita, Y. Neuronal correlate of visual associative long–term memory in the primate temporal cortex. *Nature*, 335:817–820, 1988.

[11] Palm, G. Cell assemblies as a guideline for brain research. *Concepts in Neuroscience*, 1(1):133–147, 1990.

[12] Singer, W. Search for coherence: A basic principle of cortical self-organization. *Concepts in Neuroscience*, 1(1):1–26, 1990.

[13] Haberly, L. B. Neuronal circuitry in olfactory cortex: Anatomy and functional implications. *Chem. Sens*, 10:219–238, 1985.

[14] Rolls, E. T. Principles underlying the representation and storage of information in neuronal networks in the primate hippocampus and cerebral cortex. In Zornetzer, S. F., Davis, J. L., and Lau, C., editors, *An Introduction to Neural and Electronic Networks*, pages 73–90. Academic Press, 1990.

[15] Kohonen, T. Correlation matrix memories. *IEEE Trans. Computers*, 21:353–359, 1972.

[16] Willshaw, D. J., Longuet-Higgins, H. C., and Buneman, O. P. Non–holographic associative memeory. *Nature*, 222:960, 1969.

[17] Hopfield, J. Neural networks and physical systems with emergent collective computational abilities. *Proc. Natl. Acad. Sci. USA*, 79:2554–2558, 1982.

[18] Smolensky, P. Information processing in dynamical systems: Foundations of harmony theory. In E., R. D. and McClelland, J. L., editors, *Parallel Distributed Processing (vol. 1)*, pages 195–281. The MIT Press, 1986.

[19] Lansner, A. and Ekeberg, Ö. A one-layer feedback, artificial neural network with a Bayesian learning rule. *Int. J. Neural Systems*, 1(1):77–87, 1989.

[20] Kleinfeld, D., Raccuia-Behling, F., and Chiel, H. J. Circuits constructed from identified aplysia neurons exhibit multiple patterns of persistent activity. *Biophysical J.*, 57:697–715, 1990.

[21] Smolensky, P. Connectionist modeling: Neural computation/ mental connections. In Nadel, L., Cooper, L. A., Culicover, P., and Harnish, R. M., editors, *Neural Connections, Mental Computation*, pages 49–67. Massachusets Institute of Technology, 1989.

[22] Amari, S.-I. Characteristics of sparsely encoded associative memory. *Neural Networks*, 2:451–457, 1990.

[23] Lansner, A. A recurrent Bayesian ANN capable of extracting prototypes from unlabeled noisy examples. In *Proceedings of ICANN-91*, pages 247–255, Helsinki, Finland, June 1991.

[24] Lansner, A. Information processing in a network of model neurons. A computer simulation study. Tech. Rep. TRITA-NA-8211, Dept. of Numerical Analysis and Computing Science, Royal Institute of Technology, Stockholm, Sweden, 1982.

[25] Fransén, E. and Lansner, A. Modelling Hebbian cell assemblies comprised of cortical neurons. In *Proc. Open Network Conference on Neural Mechanisms of Learning and Memory*, page 4:9, London, April 1990.

[26] Ekeberg, Ö., Stensmo, M., and Lansner, A. SWIM – a simulator for real neural networks. Tech. Rep. TRITA-NA-P9014, Dept. of Numerical Analysis and Computing Science, Royal Institute of Technology, Stockholm, Sweden, 1990.

[27] Ekeberg, Ö., Wallén, P., Lansner, A., Tråvén, H., Brodin, L., and Grillner, S. A computer based model for realistic simulations of neural networks. I: The single neuron and synaptic interaction. *Biol. Cybernetics*, 65(2):81–90, 1991.

[28] McCormick, D. A., Connors, B. W., and Lighthall, J. W. Comparative electrophysiology of pyramidal and sparsely spiny stellate neurons of the neocortex. *J. Neurophysiology*, 54(4):782–806, 1985.

[29] Kandel, E. R. and Spencer, W. A. Electrophysiology of hippocampal neurons: II. After–potentials and repetetive firing. *J. Neurophysiology*, 24:243–259, 1961.

[30] Bush, P. C. and Douglas, R. J. Synchronization of bursting action potential discharge in a model network of neocortical neurons. *Neural Computation*, 3:19–30, 1991.

[31] Grillner, S., Wallén, P., Brodin, L., and Lansner, A. Neuronal network generating locomotor behaviour in Lamprey: Circuitry, transmitters, membrane properties, and simulation. *Ann. Rev. Neurosci.*, 14:169–199, 1991.

[32] Brodin, L., Tråvén, H., Lansner, A., Wallén, P., Ekeberg, Ö., and Grillner, S. Computer simulations of N-methyl-D-aspartate (NMDA) receptor induced membrane properties in a neuron model. *J. Neurophysiol.*, 66(2):473–484, 1991.

[33] Freeman, W. and Skarda, C. Spatial EEG patterns, non-linear dynamics and perception: the neo-Scherringtonian view. *Brain Res. Rev.*, 10:147–175, 1985.

[34] Eckhorn, R., Bauer, R., Jordan, W., Brosch, W., Kruse, W., Munk, M., and Reitboeck, H. J. Coherent oscillations: A mechanism for feature linking in the visual cortex. *Biol. Cybernetics*, 60:121–130, 1988.

[35] Gray, C. M. and Singer, W. Stimulus-specific neuronal oscillations in orientation columns of cat visual cortex. *Proc. Natl. Acad. Sci. USA*, 86:1698–1702, 1989.

[36] Bower, J. M. Reverse engineering the nervous system: An anatomical, physiological, and computer-based approach. In Zornetzer, S. F., Davis, J. L., and Lau, C., editors, *An Introduction to Neural and Electronic Networks*, pages 3–24. Academic Press, 1990.

[37] Getting, P. A. and Willows, A. O. D. Burst formation in electrically coupled neurons. *Brain Research*, 63:424–429, 1973.

[38] Thorpe, S. and Imbert, M. Biological constraints on connectionist modelling. In Pfeifer, R., editor, *Connectionism in Perspective*. Springer Verlag, Berlin, 1989.

[39] Levin, B., Hammarlund, P., and Lansner, A. BIOSIM, a program for biologically realistic neural network simulations on the Connection Machine. Technical Report TRITA-NA-9021, Dept. of Numerical Analysis and Computing Science, Royal Institute of Technology, Stockholm, Sweden, 1990.

Figure 1 a: Soma membrane potential during an action potential produced by the P–cell (upper trace), the MN–cell (middle trace) and FS–cell (lower trace). Stimulation is indicated by the horizontal bar.

Figure 1 b: Representative spike trains of the P–cell (upper trace), the MN–cell (middle trace) and the FS–cell (lowe trace). The cells were driven by current stimulation of 0.4, 1.2 and 0.9 nA respectively.

Table 1: Parameters for which the P–cell differ from the MN–cell. The right–most column gives the effect on the P–cell properties relative to the MN–cell.

Figure 2: Current–frequency plot for the P–, MN– and FS–cell (steady state firing).

Figure 3 a: An assembly of P–cells displaying after–activity. Each of the fifty lowermost traces shows the intracellular soma membrane potential of the corresponding P–cell in the network simulated. The fifty uppermost traces show the FS–cells. The total time simulated was 500 ms. The eight P–cells in the assembly were stimulated with 0.4 nA for 40 ms.

Figure 3 b: An assembly of eight MN–cells stimulated with 1.5 nA for 40 ms displaying absence of after–activity. As in (a) the total time simulated was 500 ms.

Figure 4: Examples of pattern completion and competition. Only excitatory cells are displayed. In all cases, the total time simulated was 500 ms. (a) Activity of the P–cells in an assembly with two cells stimulated. (b) As in (a) but with three cells stimulated. Now pattern completion takes place. (c) An assembly of MN–cells with 7 out of 8 cells stimulated for 350 ms. (d) Competition between two assemblies of P–cells. The stimulated cells in the two different patterns are marked with open and closed circles.

Figure 5: "Synthetic field potential" and spike markings are shown for three different situations; Upper traces: Spike synchronization displayed by an assembly of MN–cells mutually connected by excitatory synapses located at the most proximal dendritic compartment. Mean value of the EPSP:s on the MN–cells and on the FS–cells were 2.8 mV and 1.5 mV respectively. The IPSP:s on the MN–cells were -2.1 mV Middle traces: The same network but with the mutual excitation removed (for control). In both cases, continuous stimulation with 1.2 nA was given. Lower traces: Results with an assembly of P–cells mutually connected by excitatory synapses.

Parameter	*Value for P*	*Value for MN*	*Unit*	*Effect*
$E_{leak_{soma}}$	-50	-70	mV	resting potential less negative
$E_{leak_{dendr}}$	-50	-70	mV	resting potential less negative
$G_{K(Ca)}$	0.0017	0.010	μS	larger DAP, smaller AHP
$G'_{K(Ca)}$	0.016	0.005	μS	larger DAP, smaller late AHP
δ_{NMDA}	2.0	3.0	s^{-1}	larger DAP, smaller late AHP
E_K	-70	-90	mV	repolarizing amplitude smaller
A_{β_n}	40	5	$mV^{-1}s^{-1}$	repolarizing amplitude smaller
B_{α_n}	-15	-31	mV	spike width smaller
B_{β_n}	-40	-28	mV	spike width smaller
G_K	0.5	0.2	μS	spike width smaller
E_{Na}	40	50	mV	spike height smaller

Table 1. Difference between the P-cell and the MN-cell*.

* the EIN-cell in the Lamprey simulations.

		Na^+		K^+	Ca^{2+}	NMDA
		m	h	n	q	p
	A ($\mathrm{mV^{-1}\,ms^{-1}}$)	0.2	0.08	0.02	0.08	0.7 ($\mathrm{ms^{-1}}$)
α	B (mV)	-40	-40	-31	-25	–
	C (mV)	1	1	0.8	1	17
	A ($\mathrm{mV^{-1}\,ms^{-1}}$)	0.06	0.4 ($\mathrm{ms^{-1}}$)	0.005	0.005	0.1 ($\mathrm{ms^{-1}}$)
β	B (mV)	-49	-36	-28	-20	–
	C (mV)	20	2	0.4	20	17

Table 2: Parameters used in describing the ion channels for MN.

		Na^+		K^+	Ca^{2+}	NMDA
		m	h	n	q	p
	A ($\mathrm{mV^{-1}\,ms^{-1}}$)					
α	B (mV)	-30	-30	-21	-15	
	C (mV)		0.2	0.2		
	A ($\mathrm{mV^{-1}\,ms^{-1}}$)			20		
β	B (mV)	-39	-26	-18	-10	
	C (mV)		0.2	0.2		

Table 3: Parameters used in describing the ion channels for FS that differ from the MN–cell.

Passive Properties		Active Properties			
E_{leak}	$-70\,\mathrm{mV}$	E_{Na}	$50\,\mathrm{mV}$	ρ_{AP}	$4\,\mathrm{s^{-1}\,mV^{-1}}$
G_m Soma	$0.0032\,\mu S$	G_{Na}	$1.0\,\mu S$	δ_{AP}	$75\,\mathrm{s^{-1}}$
C_m Soma	$0.032\,\mathrm{nF}$	E_K	$-90\,\mathrm{mV}$	ρ_{NMDA}	$1.107{*}10^6{*}G_{NMDA}\,\mathrm{s^{-1}\,mV^{-1}}$
G_m Dendrites	$0.0096\,\mu S$	G_K	$0.2\,\mu S$	δ_{NMDA}	$3\,\mathrm{s^{-1}}$
C_m Dendrites	$0.288\,\mathrm{nF}$	E_{Ca}	$150\,\mathrm{mV}$	E_{NMDA}	$0\,\mathrm{mV}$
G_{core}	$0.04\,\mu S$	G_{Ca}	$0\,\mu S^{\dagger}$	G_{NMDA}	see text μS
t_{delay}	1 ms	$G_{K(Ca)}$	$0.01\,\mu S$	E_{Na+K}	30 mV
$t_{duration}$	3 ms	$G'_{K(Ca)}$	$0.005\,\mu S$	E_{Cl}	-85 mV
				$E_{Ca(NMDA)}$	20 mV

Table 4: Parameters used for the MN simulations in this paper. The parameters correspond to those of excitatory interneurons in the simulations of the spinal locomotor network of the lamprey. †The current contribution of the Ca^{2+} ions is negelected.

Passive Properties		Active Properties			
G_m Soma	$0.0016\,\mu S$	G_K	$1.0\,\mu S$	ρ_{AP}	$0.013\,\mathrm{s^{-1}\,mV^{-1}}$
C_m Soma	$0.016\,\mathrm{nF}$			δ_{AP}	$20\,\mathrm{s^{-1}}$
G_{core}	$0.0638\,\mu S$				

Table 5: Parameters used for the FS–cell that differ from the MN–cell.

MODELLING HEBBIAN CELL ASSEMBLIES COMPRISED OF CORTICAL NEURONS

Short title: Modelling Hebbian Cell Assemblies

A. Lansner, E. Fransén
SANS—Studies of Artificial Neural Systems
Dept. of Numerical Analysis and Computing Science
Royal Institute of Technology, S–100 44 Stockholm, Sweden
E–mail: ala@sans.kth.se

Scanned Figures

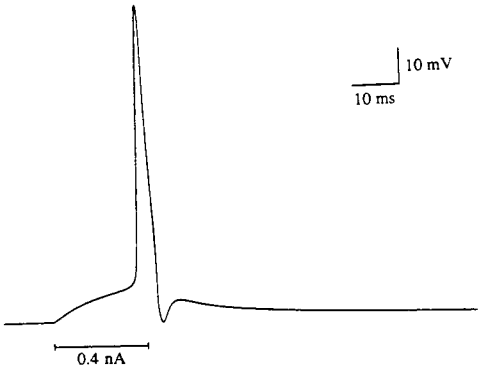

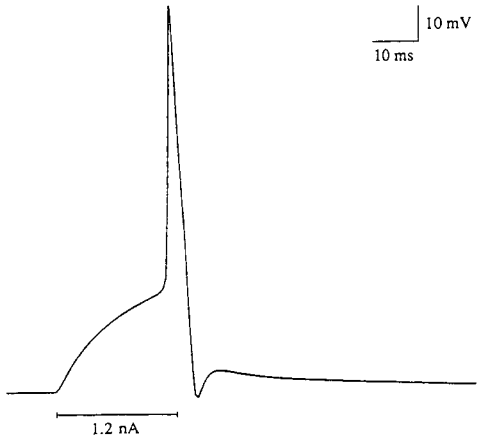

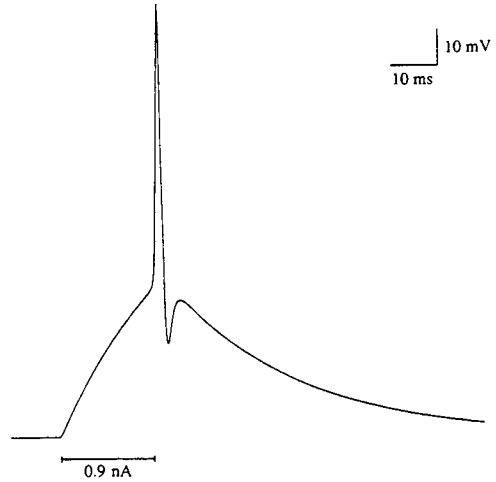

Figure 1. Soma membrane potential during an action potential produced by the P-cell (upper trace), the MN-cell (middle trace) and FS-cell (lower trace). Stimulation is indicated by the horizontal bar.

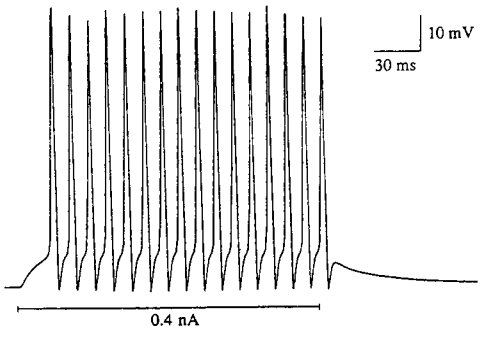

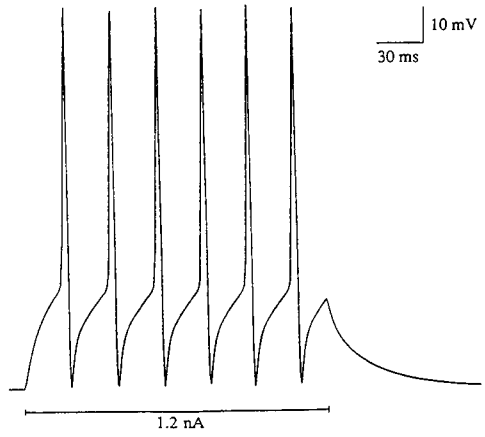

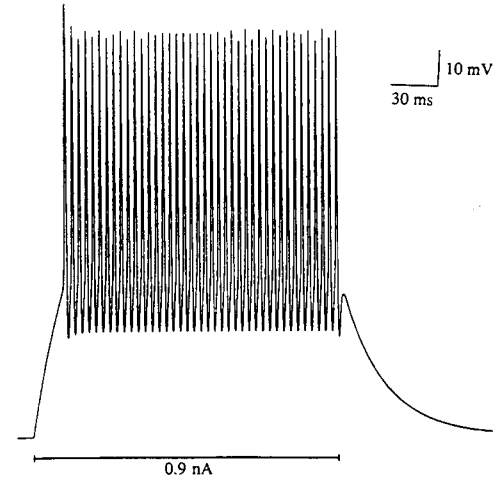

Figure 2. Representative spike trains of the P-cell (upper trace), the MN-cell (middle trace) and the FS-cell (lower trace). The cells were driven by current stimulation of 0.4, 1.2 and 0.9 nA respectively.

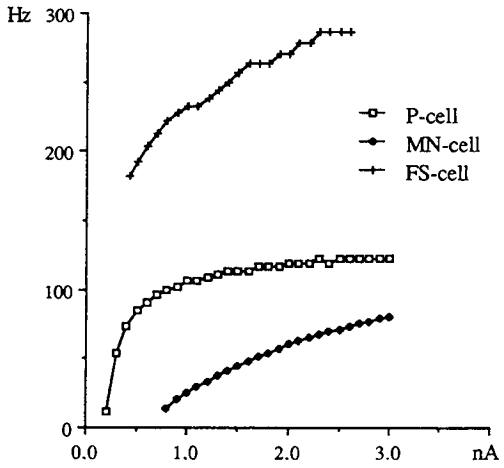

Figure 3. Current–frequency plot for the P-, MN- and FS-cells (steady state firing).

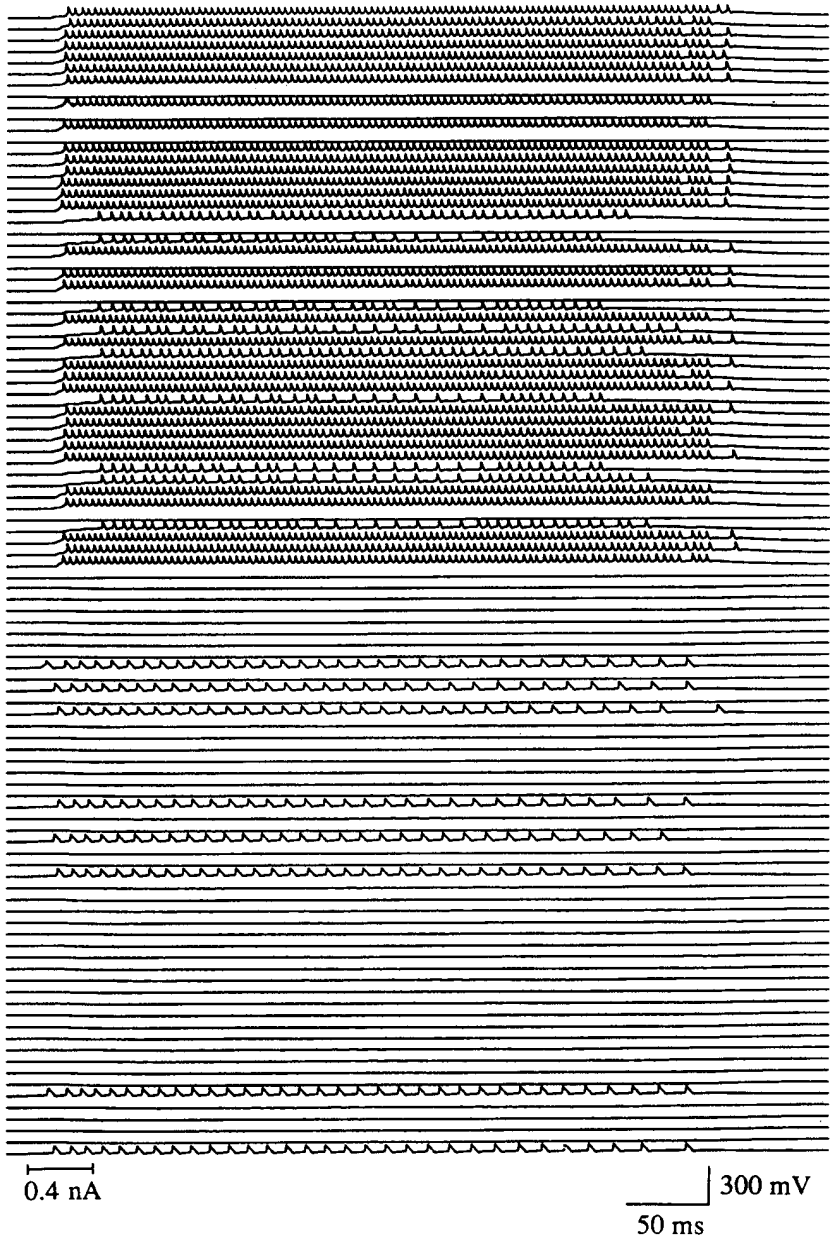

Figure 4. An assembly of P-cells displaying after-activity. Each of the fifty lowermost traces shows the intracellular soma membrane potential of the corresponding P-cell in the network simulated. The fifty uppermost traces show the FS-cells. The total time simulated was 500 ms. The eight P-cells in the assembly were stimulated with 0.4 nA for 40 ms.

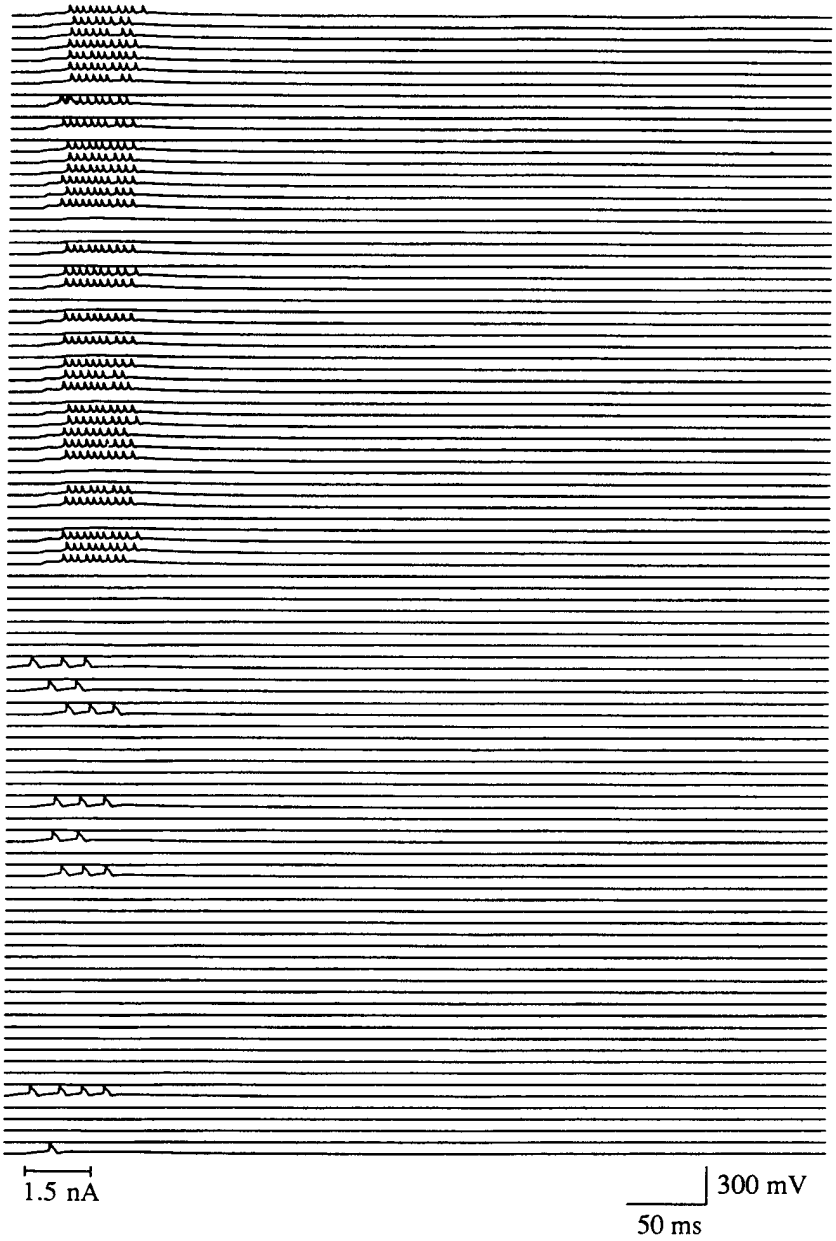

Figure 5. An assembly of eight MN-cells stimulated with 1.5 nA for 40 ms displaying absence of after-activity. As in figure 4 the total time simulated was 500 ms.

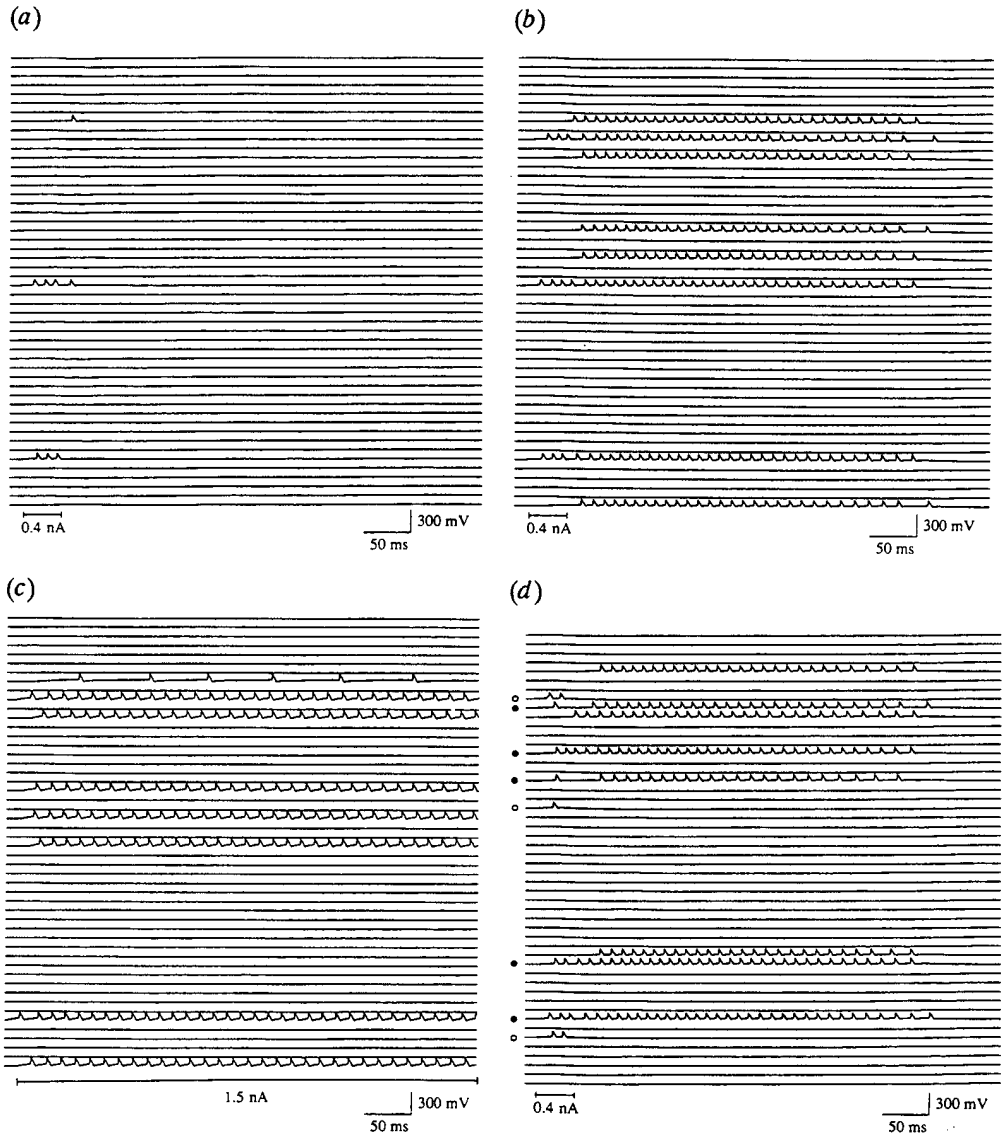

Figure 6. Examples of pattern completion and competition. Only excitatory cells are displayed. In all cases, the total time simulated was 500 ms. (*a*) Activity of the P-cells in an assembly with two cells stimulated. (*b*) As in (*a*) but with three cells stimulated. Now pattern completion takes place. (*c*) An assembly of MN-cells with seven out of eight cells stimulated for 350 ms. (*d*) Competition between two assemblies of P-cells. The stimulated cells in the two different patterns are marked with open and closed circles.

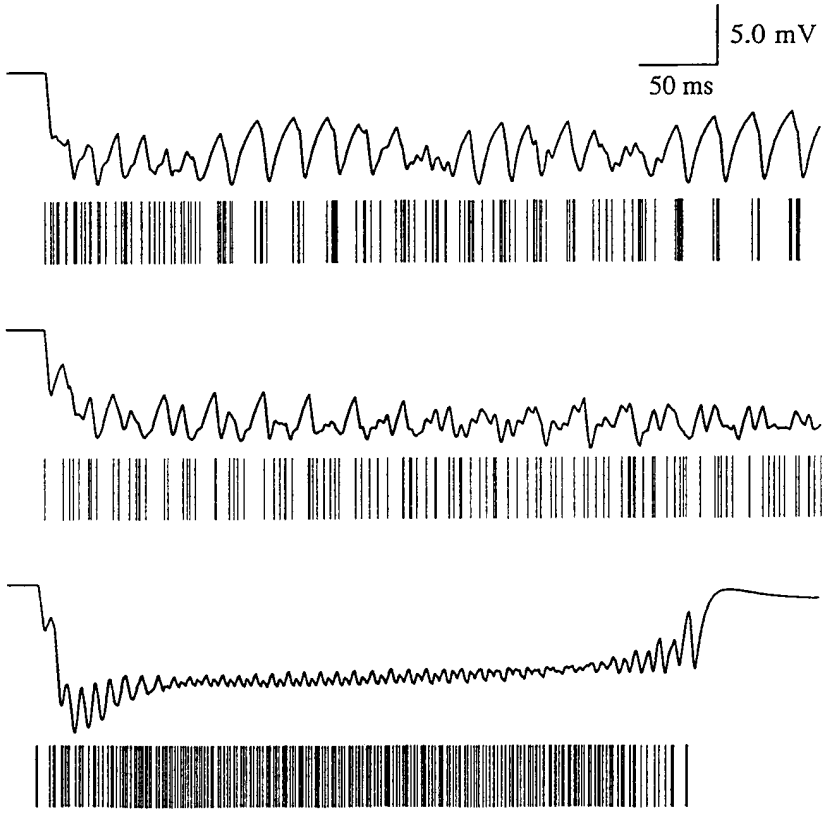

Figure 7. 'Synthetic field potential' and spike markings are shown for three different situations. Upper traces: Spike synchronization displayed by an assembly of MN-cells mutually connected by excitatory synapses located at the most proximal dendritic compartment. Mean value of the EPSPs on the MN-cells and on the FS-cells were 2.8 mV and 1.5 mV respectively. The IPSPs on the MN-cells were −2.1 mV. Middle traces: The same network but with the mutual excitation removed (for control). In both cases, continuous stimulation with 1.2 nA was given. Lower traces: Results with an assembly of P-cells mutually connected by excitatory synapses.